An Integrated Sensing System for Monitoring the Corrosion Activity in Concrete Blocks Exposed at Hangzhou Bay Bridge

Second Conference on Smart Monitoring,
Assessment and Rehabilitation of Civil Structures

SMAR 2013

An Integrated Sensing System for Monitoring the Corrosion Activity in Concrete Blocks Exposed at Hangzhou Bay Bridge

Sudarshan Srinivasan[1], P.A. Muhammed Basheer[1], Jiang-Hong Mao[2], Wei-Liang Jin[3] and W John McCarter[4]

[1] School of Planning, Architecture and Civil Engineering, Queen's University Belfast, Belfast, United Kingdom
[2] Ningbo Institute of Technology, Zhejiang University, Ningbo, P.R.China
[3] Institute of Structural Engineering, Zhejiang University, Hangzhou, P.R.China
[4] School of Built Environment, Herriot-Watt University, Edinburgh, United Kingdom

ABSTRACT: This paper discusses the importance of integrated sensing systems comprising techniques that give different types of data from a structure exposed to the marine environment so that its service life could reliably be predicted. For this purpose, a novel sensor combination was designed and installed in concrete panels which were exposed to Hangzhou Bay Bridge in China. The integrated sensor probe was used to monitor the cover concrete as well as the reinforcement. The sensor probes were connected to a monitoring station, which enabled access and control of the data remotely from Belfast, UK. The initial data obtained from the monitoring station gives interesting information on the early age properties of concrete and distinct variations in these properties with different types of concrete. This paper also reports the variation in electrical properties of different concrete samples and environmental data in response to the marine exposure condition at Hangzhou bay bridge.

1 INTRODUCTION

Concrete structures in marine environments are exposed to extreme environmental conditions, such as salt induced corrosion, abrasion and various types of physical and chemical damages due to both sea water and cyclic wetting and drying. The corrosion of reinforcement is one of the major contributors of damage in reinforced concrete structures exposed to marine environment. In general, corrosion of reinforcement due to carbonation, chloride ingress and/or leaching accounts for more than 50% of the reported cases of durability issues of reinforced concrete structures (BCA 1997). Therefore, maintaining marine structures from corrosion induced damage continues to be a major challenge for civil engineers in the 21st century. Although there are well established guidelines and standards to specify, design and construct these structures, including specifications for materials, corrosion protection systems and maintenance management, they deteriorate prematurely due to poor workmanship, lack of quality control of materials and constraints on the budget. Therefore, it is highly desirable to assess the likely performance of a structure soon after its construction is finished and continuously monitor the performance throughout its service life.

During the construction phase, concrete in its fresh state undergoes complex chemical reactions between cementitious materials and water, which determines the later age properties such as porosity, pore structure formation, and mechanical and durability properties (McCarter and Curran 1984, McCarter et al. 2003, McCarter et al. 2005). During the hydration process physical

and chemical changes take place in the microstructure of concrete, which include ion dissolution, decrease in porosity due to the formation of new chemical compounds, rise in temperature caused by exothermic reactions of hydration, micro-structural development and pore formation due to evaporation of water (Hewlett, 2003). The quality and performance of early age concrete can be assessed by monitoring the rate of hydration reactions and variations in micro-structure, moisture and temperature distributions (McCarter et al, 2005). Therefore, the information gathered by continually monitoring these early age characteristics (initially until 28 days of age) can help in understanding the curing process, setting behaviour, pore structure and strength development of the concrete. In later ages (after 28 days), the strength development of concrete slows down and concrete in the cover zone tends to equilibrate with the surrounding environmental conditions.

When concrete structures are exposed to extreme conditions in the marine environment, initial deterioration of the cover concrete can instigate other deterioration processes, which, if unnoticed, can result in the damage to the whole structure. Therefore, the quality of cover concrete in marine environments needs to be continually monitored so as to identify the initiation of deterioration before the process aggravates and causes damage to the structure. Moreover, the continuous monitoring of the cover concrete will help with data which can be used for predicting the in-service performance of concrete, rate the deterioration at a particular exposure condition and act as a precursor warning system for durability related damage of structures (Chrisp et al. 2002).

The deterioration of concrete in marine environments is a complex process involving the rapidly changing environmental factors along with the influence of inherent properties of concrete. In most cases of monitoring these phenomena researchers have used a specific type of sensor to identify each associated deterioration process in concrete separately. For example, anodic ladder sensors are widely used to monitor the level of corrosion at different depths in the cover zone of concrete (Raupach and Schiessl 1997). However, in order to monitor the causes and processes of the corrosion activity, a combination of sensor techniques is needed so that a better understanding of the factors involved in the deterioration of concrete can be obtained. The work reported in this paper has used an integrated sensor system consisting of electrical resistance based sensors in combination with corrosion sensors to monitor the properties of concrete at the cover zone as well as the susceptibility to corrosion of rebars. This type of sensor system is helpful to monitor the cover zone properties during the early and later ages of hydration of cementitious materials. The scope of this research work is to study the early age and long-term properties of concrete samples exposed to the marine environment at Hangzhou Bay Bridge in China by continually monitoring the spatial and temporal changes in electrical resistance, temperature and corrosion current at the cover zone of concrete using the integrated sensor system. In this paper the procedure followed in embedding the sensors in concrete samples, installation of concrete samples at field monitoring station at Hangzhou Bay Bridge, installation of data acquisition and remote data management system and the initial results obtained during the concrete manufacturing, curing and exposure phases are described.

2 SENSOR PROBE DESIGN

The integrated sensor system consisted of three different sensors, viz. array of 2-pin electrical resistance sensors, temperature sensors and a corrosion sensor. The sensor probe, as shown in Fig-1, consisted of an array of 2-pin electrical resistance sensors arranged in a staggered manner, electrical resistance based temperature sensors or thermistors and a galvanic cell corrosion sensor.

Fig-1: Sensor probe fixed in a wooden mould before pouring concrete

The staggered emplacement of 2-pin electrical resistance sensors was used to monitor the electrical resistivity or conductivity changes at different depths in the cover zone of concrete. These sensors measured the moisture and ionic movement in terms of the electrical resistance or dielectric properties of the material, which varied with moisture and ionic concentration at a constant temperature. The relationship of electrical resistance with moisture content of building materials was first described by Knowler in 1927, who also explained that unlike in DC based measurements, AC measurements have negligible disturbance caused due to polarisation of electrodes (Knowler 1927). The electrical property measurement had been used to study the hydration and microstructural evolution of cement based material systems (McCarter & Curran 1984; Wilson & Whittington 1990; Christensen et al. 1994; Levita et al. 2000; Xiao & Li 2008). Electrical conduction in concrete occurs primarily due to mobility of ions in the pore solution. Therefore, monitoring the electrical resistivity or conductivity of pore solution during early age of concrete helps in understanding the hydration, setting behaviour and microstructural variations in cement based systems. The measurement of electrical properties had been used to study various properties in concrete, such as moisture absorption-desorption characteristics (McCarter & Garvin 1989; Mccarter et al. 1995; Rajabipour et al. 2004) pozzolanic reactivity of supplementary cementitious materials (W J McCarter et al. 2003) and transport properties in cover zone of concrete (Rajabipour et al. 2004; McCarter et al. 2000; Basheer et al. 2002; McCarter et al. 2005).

The temperature sensors placed at different depths helps in monitoring the thermal gradient in the cover zone of concrete. The temperature data obtained from the concrete can also be used to predict the early age strength of concrete using maturity functions. In addition, the temperature measurements are useful to do temperature corrections on the electrical resistivity data. The corrosion sensor in the integrated sensor probe, as shown in Fig-1, can act as a precursor to the corrosion of reinforcement in concrete structure. Therefore, the corrosion sensor data serves as a warning signal before the main reinforcement in the concrete starts to corrode. The monitoring data obtained from different sensing techniques, if placed together, would provide better information on the material properties of concrete in the cover zone. The history of information gathered from these sensors would be particularly helpful in understanding the key factors involved in the deterioration of concrete structures.

3 DATA ACQUISITION AND MONITORING SYSTEM

The monitoring system for the integrated sensor probe needs a robust data acquisition unit which is capable of handling different measurement systems, able to acquire data from multiple sensor probes and sustain the long-term monitoring needs for marine structures. A custom based control

and monitoring station was designed to integrate the measurement devices. In addition to monitoring the changes in material properties and the corrosion activity in the cover zone of concrete, a weather station was installed near to the exposure site to monitor the environmental parameters such as temperature, relative humidity and wind speed. The monitoring of concrete cover zone in conjunction with the surrounding weather conditions would help in understanding the influence of environmental factors on the deterioration of concrete. The control unit for the weather station was integrated with the above mentioned custom based monitoring station such that all the sensing techniques were controlled and monitored simultaneously, as shown in the schematic in Fig-2.

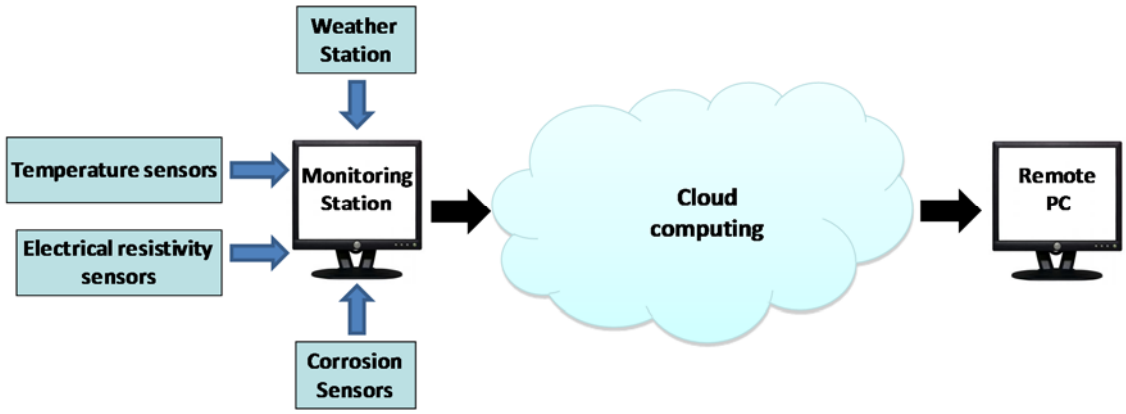

Fig-2: Schematic of the concrete monitoring station

The data obtained from different sensing techniques at the monitoring station was transmitted to a remote PC using cloud computing, as depicted in Fig-2. In addition, using the cloud computing software and the internet, the data could easily be accessed from anywhere in the world.

Table 1 Summary of concrete mixes

	HPC	**C40**	**C30**
W/C	0.36	0.45	0.56
PC (kg/m^3)	170	439	351
GGBS (kg/m^3)	85	-	-
Flyash (kg/m^3)	170	-	-
Fine Aggregate (kg/m^3)	742	571	650
Coarse Aggregate (kg/m^3)	1024	1161	1157
Superplasticiser (kg/m^3)	4.25	-	-
Slump (mm)	100	40	60

4 EXPERIMENTAL DETAILS

4.1 Materials, Sample Preparation and Curing

In the current experimental programme three different types of concrete were monitored, viz., a High Performance Concrete (HPC) and two grades (C40 and C30) of normal concrete. The mix details of the three concrete types are given in Table-1. The HPC mix used in this experimental programme is similar to the concrete mix used for the piles and pile caps of the Hangzhou Bay Bridge. The C40 mix is similar to that in the pier of the bridge, whereas the C30 mix is a high water-cement ratio mix which is widely used for ordinary constructions in China. Moreover, the C30 concrete was chosen as a low quality mix which would show some deterioration or corrosion in a short period of time in comparison to the other two mixes.

The concrete samples took the form of a slab of dimensions 350 x 300 x 150 mm. The sensor probe was fixed at the centre of the inside face of the mould, as shown in Fig-1, by means of a screw drilled through the plywood formwork from the outside. This method of emplacement of the multi-electrode sensors can easily be adapted for monitoring *in-situ* concrete by tying the two arms of the sensor probe, as shown in Fig-1, to the main reinforcement at the time of its construction. In this emplacement, the 2-pin electrode array would be in the cover zone of concrete and thus monitor the ingress of moisture or other ionic movements in the cover zone.

The moulds were filled with concrete in three layers of 50mm depth and each layer was compacted using a table vibrator. The concrete samples were de-moulded after 24 hours of casting and then they were covered with a damp hessian cloth. The samples were cured by spraying water from the main supply line on the surface once every day for a period of 4 days, which was similar to the curing regime used for the concrete in the Hangzhou Bay Bridge. After curing the samples in the laboratory for the first 4 days, the samples were wrapped in polythene sheet to avoid any evaporation of moisture and were transported to the marine exposure site at the Hangzhou Bay Bridge. The concrete samples were unwrapped at an age of 5 days whilst they were at the top deck of the marine exposure site and the side faces (350 x 150mm) of the samples were coated with an epoxy paint in 3-layers to restirct the ingress of sea water through the mould finished 350 x 350 mm face of the samples.

4.2 Marine Exposure Site – Location and Conditions

The Hangzhou Bay Bridge is one of the longest trans-oceanic bridges in the world, which is 35.6 km (22 miles) long and was completed in 2007. The bridge connects the municipalities of Jiaxing and Ningbo at Zhejiang Province in China. A service station containing shops and restaurants along with a viewing tower was built at the middle length of the bridge. A marine exposure station, shown in schematic in Fig-3, was constructed at the service station for studying both the performance of concrete and the corrosion of reinforcement in the bridge in this extreme marine environment. The environmental conditions at the bridge are quite extreme, with tidal variations of up to 9m height, which is one of the highest tidal variations in the world, and waves travelling at a speed of 30 kmph along with heavy winds.

The concrete samples embedded with sensors were placed at four different levels, as shown in Fig-3. In each level one slab each of HPC, C40 and C30 concretes were placed. Therefore, the concrete samples at level-1 were in the atmosphere zone, those at level-2 were in the splash zone and those at levels 3 and 4 were in the tidal zone. The concrete samples were fixed by bolting them firmly to the platform so as to avoid any movement or abrasion caused by the waves and tidal variations. The cables coming out from the concrete samples were properly protected by encasing them in flexible PVC pipes and the cables tied to the structure at regular intervals to avoid any movement due to tides. The tail ends of the cables were connected to the monitoring station placed at level-1, as shown in Fig-3. The weather station was placed close to the concrete samples at level-2 in the splash zone to record the temperature and moisture changes in the splash zone. The rain gauge of the weather station records the amount of sea water splash occurring at level-2. The control unit at the monitoring station was programmed to acquire data from different sensing techniques in the integrated sensor probes and transmit the data wirelessly to remote locations using cloud computing.

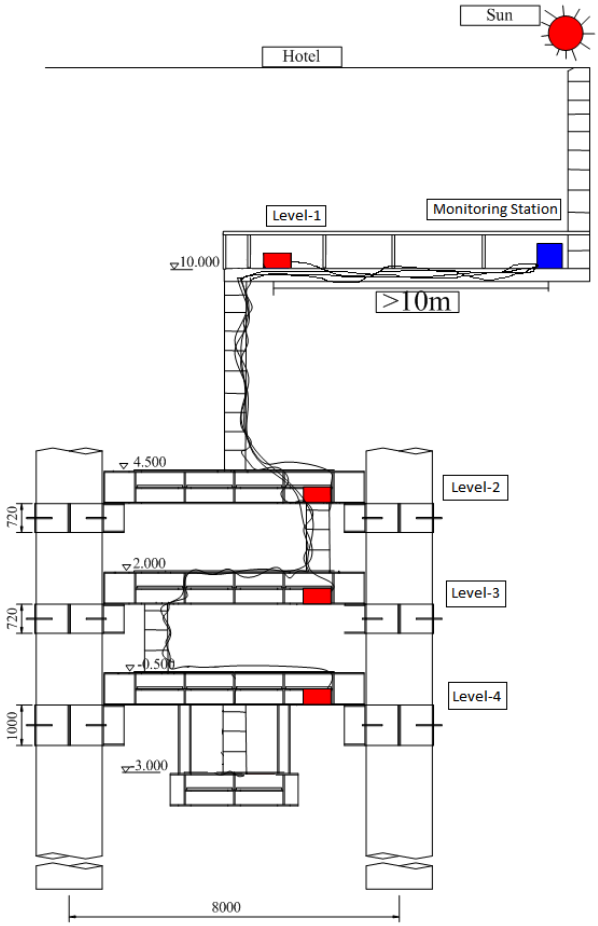

Atmospheric zone: above +10.210 m
Splash zone: +1.880～+10.210 m
Tide zone: -4.560～+1.880 m
Underwater zone: below -4.560 m

Fig-3: Schematic representation and photograph of the marine exposure site at Hangzhou Bay Bridge

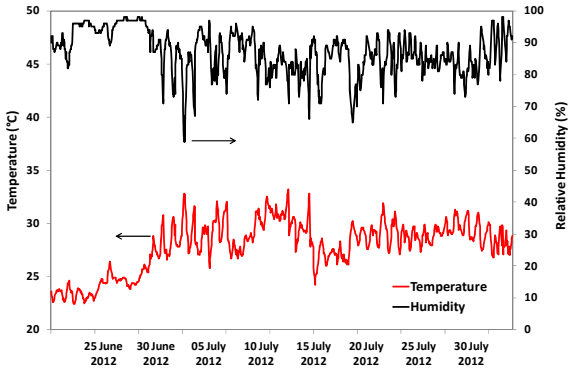

Fig-4a: Variations in Temperature and Humidity at the Hangzhou Bay bridge exposure site

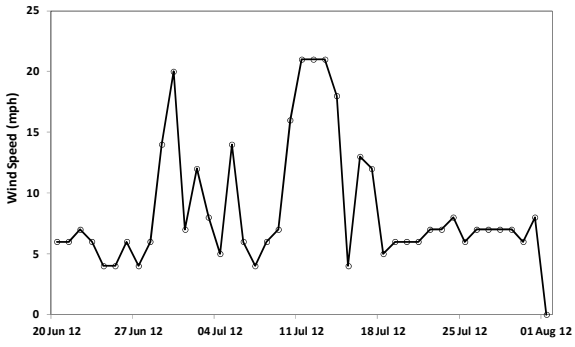

Fig-4b: Variations in daily maximum wind speed at the Hangzhou Bay bridge exposure site

The weather data obtained from the marine exposure site has been programmed to display the weather conditions live on a web page. The recent data obtained from the weather station placed at the exposure site is shown in Figs- 4a & 4b. It can be observed from the weather monitoring during Jun – Aug'12 period that there existed cyclic variations in temperature and humidity at the exposure site. The daily maximum wind speeds data shown in Fig-4b also indicate a similar trend.

4.3 Data Acquisition and Analysis

All the instrumented concrete samples in this study were connected to the monitoring system before concrete was poured into the moulds. The changes in electrical resistance and temperature during the casting and curing phases of concrete were monitored continually. The data acquisitions from all the concrete samples were programmed to be collected at every 5 minutes during the curing period of 4 days in the laboratory. During each data acquisition the electrical resistance values at six different depths, viz. 10, 20, 30, 40, 50 and 80mm from the surface and temperature at four different depths, viz. 10, 30, 50 and 80mm in the cover zone were measured for each concrete sample. As the hydration reaction of concrete changes the electrical resistance and temperature measured at different depths in the concrete, the effectiveness of concrete curing was assessed using this technique.

The electrical resistance measured at different depths using the 2-pin electrode array was converted to electrical resistivity using the following relationship:

$$\rho = c_f R \quad k\Omega\text{-cm} \qquad (1)$$

where ρ is in kΩ-cm, R is in kΩ and c_f is a calibration factor.

The calibration factor was obtained by establishing a relationship between the 4-point electrical resistance and the 2-pin electrical resistance measurements on concrete samples as reported elsewhere by one of the authors (McCarter et al. 2009). The calibration factor for a similar electrode configuration used in the present work was determined as 2.43 cm (McCarter et al. 2012).

5 RESULTS AND DISCUSSIONS

5.1 Early age concrete monitoring

In this investigation three different concrete mixes with different water-binder ratios were tested. The changes in electrical resistivity at different depths with time for the C30 concrete during the first four days of curing are shown in Fig-5a. It may be noted that these data were collected at Belfast from the slabs manufactured in China using the remote monitoring set up described in section 3

Based on the trend observed in Fig-5a the graph can be divided into three phases, the first phase is the initial 3 hrs of hydration, the second phase is from 3-24 hrs of hydration and the third phase is from 24-100 hrs of hydration. It can be observed from Fig-5a that during the first phase there is not much change in electrical resistivity values as the ions which conduct electricity between the electrodes are readily available due to the fresh state of concrete. In the second phase, as the concrete begins to set and changes into a semi-solid state the resistivity values increase rapidly with time. The changes in resistivity of concrete in the second phase mainly depend on the pore structure formation. In the third phase, as the concrete hardens completely the electrical resistivity measured at different depths tends to stabilise with time and the value at which this occurs normally depends on the type of concrete and degree of hydration (i.e. effect of curing).

Fig-5b shows the temperature changes at both 10 mm and 80 mm depths for C30 concrete. It is evident from this figure that the temperature in concrete increased with time for the initial 12 hours due to the exothermic hydration reactions. In addition, the temperature values at 80 mm depth are marginally greater than the temperature measured at 10 mm depth initially, but both were similar after around 2 days, which is mainly due to the influence of ambient room temperature at shallow depths.

The changes in electrical resistivity and temperature for the C40 concrete are shown in Fig-6a and 6b respectively. The trend in the changes in resistivity values observed for the C40 concrete is similar to that for the C30 concrete. The rate of changes in resistivity observed in the initial part of the second phase is greater for the C40 concrete when compared to the C30 concrete. The increase in temperature in Fig. 6b for the C40 concrete is slightly greater than that for the C30 concrete in Fig. 5b. This is considered to be due to increased degree of hydration of cement because the C40 concrete had more cement content compared to the C30 mix.

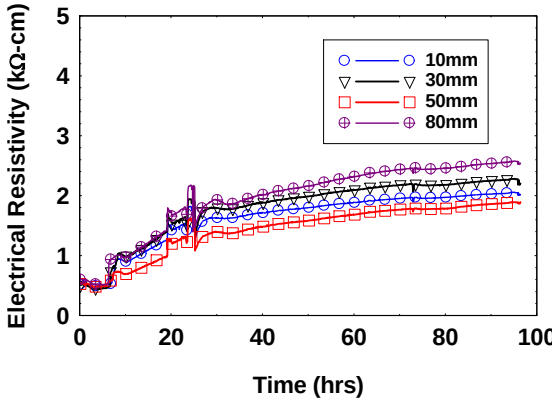

Fig-5a: Changes in electrical resistance at different depths with time for C30 Concrete

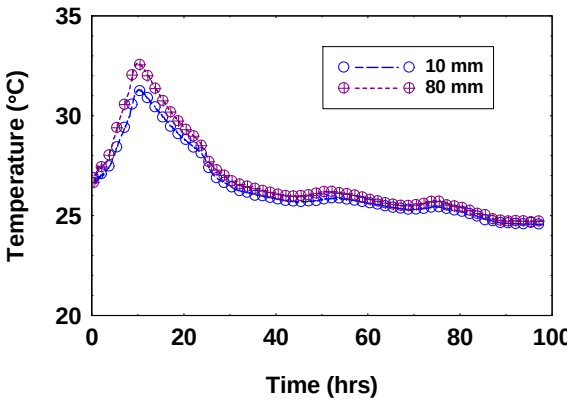

Fig-5b: Changes in temperature at different depths with time for C30 concrete

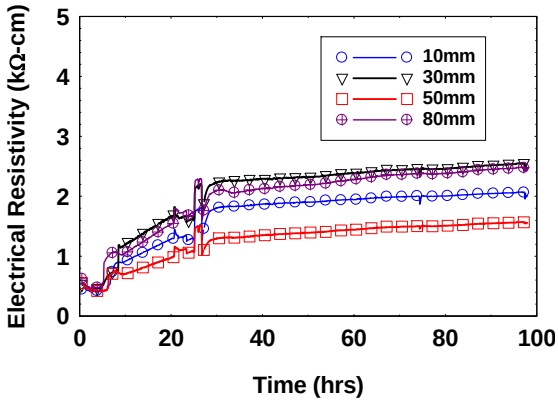

Fig-6a: Changes in electrical resistance at different depths with time for C40 Concrete

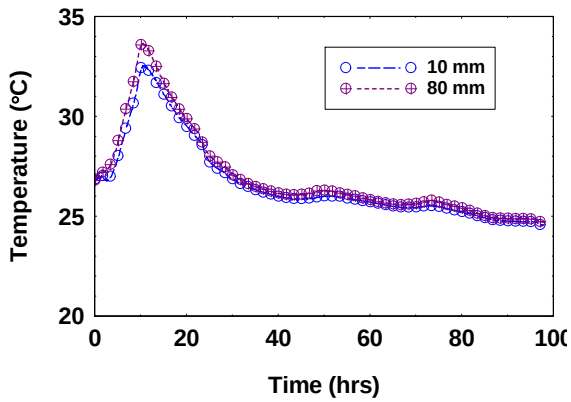

Fig-6b: Changes in temperature at different depths with time for C40 concrete

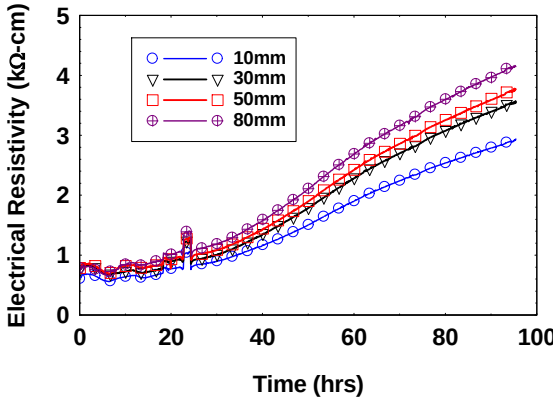

Fig-7a: Changes in electrical resistance at different depths with time for HPC

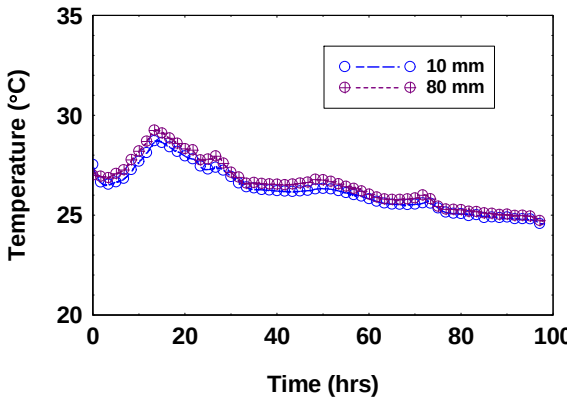

Fig-7b: Changes in temperature at different depths with time for HPC

The resistivity and temperature plots for the HPC are shown in Fig-7a and 7b respectively. The resistivity changes observed for HPC clearly show a distinct feature of prolonged increase in the third phase when compared to both C30 and C40 concretes. This increase in electrical resistivity at different depths is attributed to the slow pozzolanic reaction and better pore structure in the HPC. Moreover, the rapid increase of resistivity in the second phase is not observed in the case of the HPC due to the slow pozzolanic reaction of fly ash and GGBS in the concrete. The increase in temperature for the HPC as shown in Fig-7b is low in comparison to that for both C30 and C40 concretes. This is attributed to the low heat of hydration of HPC containing supplementary cementitious materials in the concrete mix.

The electrical resistivity values for fresh concrete were generally low (Figs. 5a, 6a and 7a) due to the high conduction through dissolved ions in the fresh state of concretes. As the cement in the concrete hydrates with time the concrete hardens slowly depending on the cement content, water-binder ratio and the content of the supplementary cementitious materials in the concrete mix, which in turn increases the electrical resistivity measured at different depths in the concrete. At the hardened phase of concrete the electrical resistivity values depends on the pore structure formation, pore connectivity and constituents of the pore solution in the concrete. Both the temperature and the electrical resistivity data obtained from the sensors were useful to differentiate the mixes.

5.2 Later age concrete monitoring (after 28 days)

After the concrete samples were cured in the laboratory for initial 4 days the samples were transported to the exposure site at Hangzhou Bay Bridge. All the concrete samples were initially placed in level-2 of the exposure platform (Fig-3) and the cables were connected to the monitoring station installed at Level-1. When the concrete was 7 days of age, one concrete block in each concrete type was installed at four levels of the exposure platform (Fig-3). Fig-8 shows the variations in electrical resistance ratio, ρt/ρ28, which is the ratio of electrical resistivity of concrete measured at time 't' to electrical resistivity measured at 28 days. Presented in Figs-8a, 8b and 8c are the electrical resistance data obtained from three different concrete blocks placed at level-1 (atmosphere zone). It can be seen from Fig-8a that the electrical resistivity ratio at different depths for C30 concrete increased with time, which was higher at the 10mm depth in comparison to measurement made at 30, 50 and 80mm depths. The latter trend can be attributed to the drying or evaporation of moisture at surface due to surrounding environmental conditions at level-1.

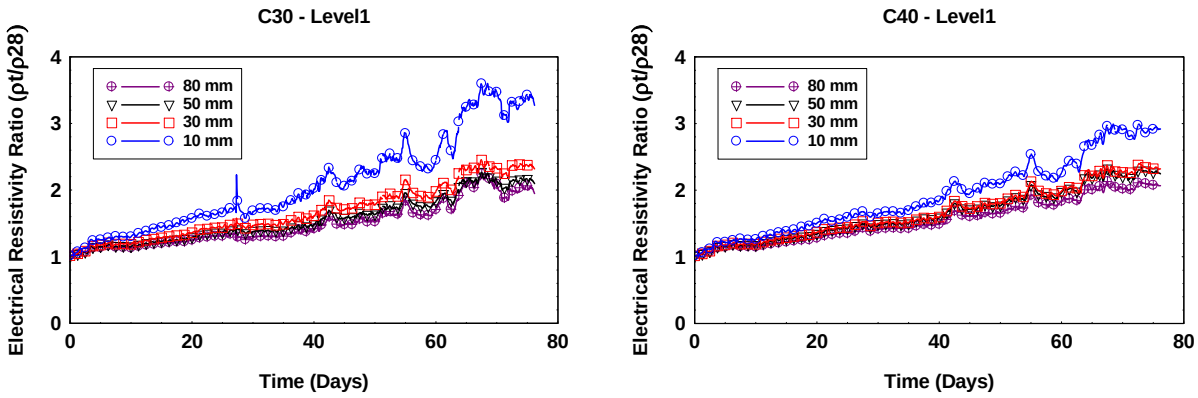

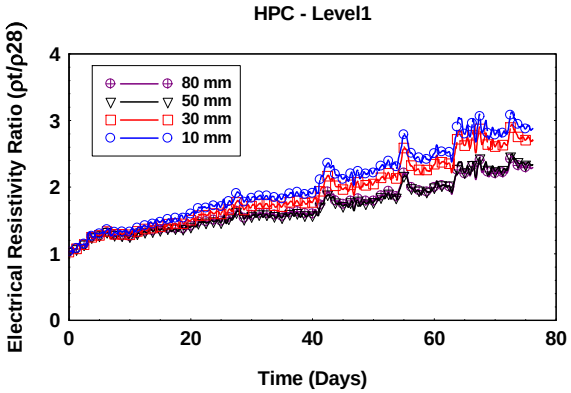

Fig-8 Variations in electrical resistivity ratio of concrete at different depths with time

Fig.8a – C30 concrete

Fig.8b – C40 concrete

Fig.8c – HPC

The results in Figs-8b and 8c also show an increase in the resistivity ratio with time for the C40 concrete and HPC respectively. The larger increase in electrical resistivity ratio at 10mm depth for the C30 concrete compared to both C40 concrete and HPC would suggest that there was higher rate of drying at surface for the former compared to the other two. The increased rate of drying at surface for C30 concrete is mainly due to high W/C ratio for C30 concrete, resulting in relatively high porosity and thus facilitating easy evaporation of moisture at surface.

6 CONCLUSIONS

The work presented highlights the usefulness of integrated sensor systems for assessing the properties of concrete in the cover zone and predicting the remaining service life. An advanced remote monitoring station was developed and instrumented at the Hangzhou bay bridge in China, which enabled monitoring and access of information on concrete performance remotely from Belfast, UK. In this research work the external environmental conditions at the exposure site was monitored in conjunction with the internal properties in the cover zone of concrete. This work also highlights the importance of measuring electrical properties and temperature of the cover zone of concrete, which can be used to assess the effectiveness of curing, rate of hydration and pore structure formation during the early ages of concrete. The investigation carried out in monitoring spatial distribution of electrical resistivity and temperature with time for different concrete mixes has led to the following conclusions:

- The electrical resistivity changes monitored for the C30, C40 and high performance concretes have shown three different phases during their early ages of hydration. The initial phase lasted until the concrete stiffened, the second phase coincided with the development of pore structure as a result of hydration during 3-24 hours and the third phase was for hydration beyond 24 hours. The temperature sensors in the integrated sensor system were able to monitor the heat evolution due to the hydration reactions in the three different concretes.
- There was prolonged increase in electrical resistivity observed for the HPC, which was absent for both C30 and C40 concretes. This is considered to be due to the influence of slow pozzolanic reaction of the supplementary cementitious materials, viz. fly ash and GGBS, in the HPC mix. The temperature data for the HPC mix clearly showed lower heat of hydration, which is considered to be due to the delayed reaction caused by the presence of the supplementary cementitious materials in the HPC mix.

- The variations in electrical resistivity ratio for concrete exposed to a dry location at the exposure site showed increased drying at the surface for C30 concrete in comparison to C40 and high performance concretes.

7 REFERNCES

Basheer, P.A.M. et al., 2002. Monitoring electrical resistance of concretes containing alternative cementitious materials to assess their resistance to chloride penetration. *Cement and Concrete Composites*, 24(5), pp.437–449.

British Cement Association, 1997. *Development of an holistic approach to ensure the durability of new concrete construction*, British Cement Association.

Chrisp, TM, McCarter, WJ & Starrs, G, 2002. Depth-related variation in conductivity to study cover-zone concrete during wetting and drying. *Cement and Concrete …*, 24, pp.415–426.

Christensen, B.J. et al., 1994. Impedance Spectroscopy of Hydrating Cement-Based Materials: Measurement, Interpretation, and Application. *Journal of the American Ceramic Society*, 77(11), pp.2789–2804.

Hewlett, P., Lea's Chemistry of Cement and Concrete, 4th edition, Butterworth Heinemann, 2003.

Knowler, A.E., 1927. The Electrical Resistance of Porous Materials. , 40, pp.37–40.

Levita, G. et al., 2000. Electrical properties of fluidified Portland cement mixes in the early stage of hydration. *Cement and Concrete Research*, 30(6), pp.923–930.

Mc Carter, W.J. & Curran, P.., 1984. The Electrical Response Characteristics Of Setting Cement Paste. *Magazine Of Concrete Research*, 36(126).

McCarter, W et al., 2012. Influence of Different European Cements (CEM) on the Hydration of Cover-Zone Concrete during the Curing and Post Curing Periods. *Journal of Materials in Civil Engineering*.

McCarter, W J et al., 2003. Characterization and monitoring of cement-based systems using intrinsic electrical property measurements. *Cement and Concrete Research*, 33(2), pp.197 – 206.

McCarter, W J & Garvin, S., 1989. Dependence of electrical impedance of cement-based materials on their moisture condition. *Journal of Physics D: Applied Physics*, 22(11), pp.1773–1776.

McCarter, W J, Starrs, G & Chrisp, T M, 2000. Electrical conductivity, diffusion, and permeability of Portland cement-based mortars. *Cement and Concrete Research*, 30(9), pp.1395–1400.

McCarter, W.J. et al., 2005. Field monitoring of electrical conductivity of cover-zone concrete. *Cement and Concrete Composites*, 27(7-8), pp.809–817.

Mccarter, W.J., Emerson, M. & Ezirim, H., 1995. Properties of concrete in the cover zone: developments in monitoring techniques. *Magazine of Concrete Research*, 47(172), pp.243–251.

McCarter, WJ, Starrs, Gerry & Kandasami, S., 2009. Electrode configurations for resistivity measurements on concrete. *ACI Materials Journal*, (106).

Rajabipour, F., Weiss, J. & Abraham, D.M., 2004. Insitu electrical conductivity measurements to assess moisture and ionic transport in concrete. In J. Weiss et al., eds. *International RILEM Symposium on Concrete Science and Engineering: A Tribute to Arnon Bentur*. RILEM Publications SARL, p. 43.

Raupach, M. and Schiessl, P., 1997, Monitoring system for the penetration of chlorides, carbonation and the corrosion risk for the reinforcement, Construction and Building Materials, 11, 207-214.

Wilson, J.G. & Whittington, H.W., 1990. Variations in the electrical properties of concrete with change in frequency. *Science Measurement and Technology IEE Proceedings A*, 137(5), pp.246–254.

Xiao, L. & Li, Z., 2008. Early-age hydration of fresh concrete monitored by non-contact electrical resistivity measurement. *Cement and Concrete Research*, 38(3), pp.312–319.